Analyst

Accepted Manuscript

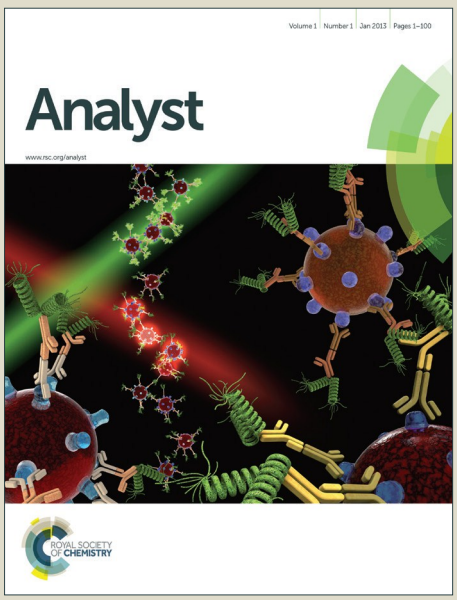

ROYAL SOCIETY OF CHEMISTRY

www.rsc.org/analyst

Journal Name

RSCPublishing

COMMUNICATION

Smartphone spectrometer for colorimetric biosensing†

Cite this: DOI: 10.1039/x0xx00000x

Yi Wang,[a,b] Xiaohu Liu,[a‡] Peng Chen,[a‡] Nhung Thi Tran,[a] Jinling Zhang,[a] Wei Sheng Chia,[a] Souhir Boujday,[a,c] Bo Liedberg*[a]

Received 00th January 2012,
Accepted 00th January 2012

DOI: 10.1039/x0xx00000x

www.rsc.org/

We report on a smartphone spectrometer for colorimetric biosensing applications. The spectrometer relies on a sample cell with an integrated grating substrate, and the smartphone's built-in light-emitting diode flash and camera. The feasibility of the smartphone spectrometer is demonstrated for detection of glucose and human cardiac troponin I, the latter in conjunction with peptide-functionalized gold nanoparticles.

Low-cost, portable sensing systems are crucial in resource-limited and remote regions of the world for medical diagnosis, environmental monitoring and nutritional examination. Commonly used sensing technologies are based on ELISA, polymerase chain reaction (PCR), mass spectroscopy (MS), surface plasmon resonance (SPR), electrochemical immunoassays and others.[1] These existing approaches have achieved high sensitivities, however, they often rely on bulky instrumentation and costly chemical procedures, requiring well-trained operators and advanced laboratory infrastructure. In developing countries, there is limited accessibility to these technologies.[2] In developed countries, despite these resources are available, the cost burden on the health care system is still a concern. Therefore, there is an urgent need for the development of low-cost portable sensing technologies that can effectively monitor and diagnose various medical conditions.[3]

To date, numerous point-of-care diagnostic devices have been developed, including microfluidic devices, plasmonic devices and paper-based devices, consumer electronic devices and so on.[4-8] Among those, optical imaging and sensing techniques based on smartphones have drawn huge attention as they can eliminate the need for bulky and costly optical instrumentation while retaining high sensitivity and image resolution. A smartphone or tablet offers an attractive and cheap alternative to bulky optical instrumentation as they take advantage of the built-in camera, screen/flash, and the connection to data storage capabilities available in the "cloud". Hence, incorporation of biosensing system into smartphone platform through the addition of different accessories is a potentially promising method to enable the smartphone to sense, transduce and communicate different types of biological information. For instance, with small field-portable fluorescence microscopy add-ons it is possible to image individual fluorescent nanoparticles and viruses with diameter down to 100 nm using a smartphone.[9] In addition, incorporation of commercially available lens systems with the smartphone enables capturing of images of cells, bacteria and biological tissue at 350× magnification.[10] Furthermore, with the attachment of a light source and a grating substrate in the front of camera, the smartphone has been used as spectrometer,[11] for label-free biosensing based on a photonic crystal substrate,[12] and portable enzyme-linked immunosorbent assays.[13] Many other optical technologies combined with smartphones also have been developed for biosensing,[8, 14] based on the measurement of transmitted intensity,[15] colour changes,[16, 17] reflectivity changes,[18] image[19-21] and fluorescence intensity.[22-24] For example, SPR has been extensively studied because of its high sensitivity to refractive index changes induced by molecular binding, thereby offering a route for real-time monitoring of molecular interactions.[25-29] Smartphone incorporated with SPR technology was reported for chemical sensing by using the screen as light source and a PDMS prism for total internal reflection.[18] Localized surface plasmon resonance (LSPR) was recently explored for bimolecular detection by monitoring the changes in transmitted light intensity through a gold nanohole array.[30] In addition, a colorimetric assay based on aggregation of aptamer-functionalized gold nanoparticles (AuNPs) was developed on a smartphone platform for the detection of mercury ions in water.[15] Despite these advances, most of these smartphone sensing platforms still require external light sources, batteries, lenses, objectives and filters, which significantly increase their size and complexity, as well as the overall cost of the accessories.

In this contribution, we demonstrate a novel standalone smartphone sensing platform that doesn't require any external light source, lens and filter. Briefly, we employ the built-in light emitting diode (LED) flash from the smartphone as the light source and the complementary metal oxide semiconductor (CMOS) camera as the detector. A compact disk (CD) with a grating serves as the dispersive unit (see the Fig. S1 in Supporting information). A schematic illustration of the smartphone sensing platform is shown in Fig. 1A. The CD grating is placed at l= 50 mm away from the LED, and slightly titled at an incident angle of α = 5º. The flash light passes through a pinhole with diameter around 1 mm attached on the front of the LED. The grating tracks are aligned normal to the incident light, and the light is then diffracted from the CD on the camera.With this setup, we detect glucose utilizing a well-known bi-enzymatic cascade assay. In addition, with peptide-functionalized AuNPs as reporters we employ the smartphone for detection of human cardiac troponin I (cTnI), a biomarker for myocardial infarction. Peptide-functionalized AuNPs recently have been widely used for detection of biomarkers,[31, 32] protease,[33] toxins,[34, 35] ions and other small molecules.[36-38] We also compare the performance of the smartphone spectrometer with a commercially available plate-reader, a bench top UV/Vis spectrometer and a LSPR spectrometer.

Since the smartphone spectrometer utilized the LED flash as the light source, it is critical to understand its spectrum. A commercial LSPR spectrometer (XNano, Insplorion, Sweden) was used to measure the spectra of light source of various smartphones, including HTC sensation XE, iPhone 5s, Nokia Lumia 920. The spectra of the flash light sources from these smartphones are virtually identical and a typical spectrum is shown in Fig. 1B. The light source covers a wavelength range from 400 to 750 nm, with two strong emission bands located at ~450 and ~550 nm, respectively (as revealed by the XNano spectrometer, black curve). In a typical measurement, the flash light was diffracted from the CD grating (640 lines/mm), and a video at frame rate of 19f/s was recorded by the CMOS camera and converted and saved as a series of images. The "rainbow" band with 570 pixels×90 pixels (Fig. 1B inset) from the selected image was then converted to an intensity spectrum using the Android software (Cell Phone Spectrometer). Briefly, to obtain the intensity spectrum profile from the image, a 90-pixel wide band was selected to yield a single intensity value for every wavelength of the spectrum (i.e. $I(\lambda)$). This process will convert one image to one intensity spectrum. Five spectra acquired from independent consecutive images were finally averaged to yield the final spectrum $A(\lambda)$, equation 1. Such a spectrum can be obtained in the wavelength range from about 430 nm to 650 nm with a wavelength resolution of 0.386 nm/pixel.

$$A(\lambda) = -\log\left(\frac{I_s(\lambda)}{I_0(\lambda)}\right), \quad (1)$$

where $I_s(\lambda)$ and $I_0(\lambda)$ are the intensity spectra of the sample and reference, respectively. A typical intensity spectrum obtained from the camera is shown in Fig. 1B (red spectrum), where three peaks are observed at ~ 450 nm, 550 nm and 600 nm, which is similar to that recorded with the XNano spectrometer (black spectrum).

We first investigated a colorimetric assay for detection of glucose based on a solution containing 2,2′-Azino-bis(3-ethylbenz-thiazoline-6-sulfonic acid) (ABTS), horseradish peroxidase (HRP), glucose oxidase (GOx). In this assay, glucose is catalytically converted (by GOx) into hydrogen peroxide, which in turn converts

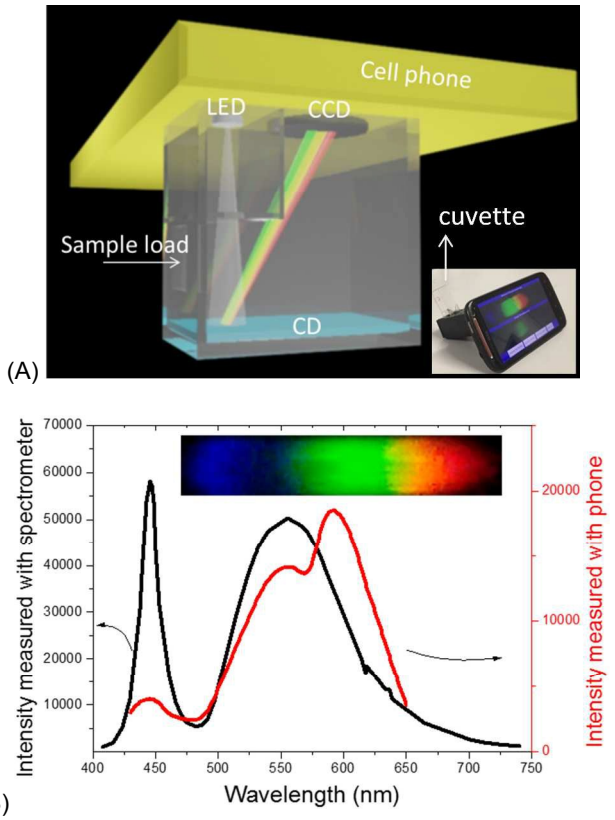

Fig. 1 (A) Schematic illustration of the smartphone spectrometer with the LED flash serving as a light source, the CMOS camera as a detector and the CD as the grating substrate. Inset: A photograph of the smartphone spectrometer. The colour band observed on the phone screen (inset and in B) is converted to the absorbance spectrum $A(\lambda)$ of the sample, eq. 1. (B) Intensity spectra of the LED light source measured by the XNano spectrometer (black) and HTC smartphone (red).

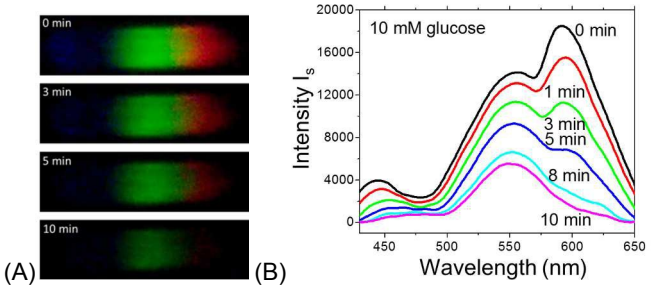

Fig. 2 (A) Colour bands of ABTS/HRP/GOx solution after incubation of 10 mM glucose for 0, 3, 5 and 10 min. (B) Intensity spectra of the samples obtained from the colour bands.

ABTS (colourless) by HRP into its oxidized form (blue). For example, in the presence of 1 mM glucose, ABTS changes colour from colourless to blue (see Fig. S2 in Supporting Information), and the absorption band appears at about 420 and 650 nm as measured by the TECAN plate-reader (Fig. S2). The optical change can also be read from the colour band with the smartphone spectrometer, see inserts Fig. 1.

Figure 2A shows the evolution of the colour bands with time in presence of 10 mM glucose. We observed an obvious decrease in the brightness for the red, green and blue bands with time. The corresponding intensity spectra in Fig. 2B confirms a gradual decrease in intensity for all the three peaks.

To compare the performance of the smartphone spectrometer with the commercial plate-reader, the absorbance for different concentrations of glucose was monitored over time. The absorbance spectra obtained from plate-reader and smartphone spectrometer indicated small difference at the wavelength around 550 nm (Fig. S3). This small difference is due to the relatively poor linear sensitivity of the smartphone to light intensity in this wavelength range as compared with the detector in plate-reader. However, monitoring the intensity changes in real-time with the smartphone spectrometer reveals its applicability in biosensing. Figure 3A and 3B show the time-dependent absorbance changes of the sample in the presence of 0.1 to 50 mM glucose measured by the TECAN plate-reader and the smartphone spectrometer, respectively. For low concentrations (0.1 to 10 mM), both of them show essentially a linear response with time. However, at high concentration of glucose (20 and 50 mM) the absorbance values measured by the smartphone spectrometer become saturated at 8 and 5 min, respectively. This is due to the strong absorption of the sample solution resulting in low intensity of light captured by the camera. The calibration curves for glucose measured by smartphone spectrometer and plate-reader are shown in Fig. 3C, with the slope of 0.053 mM^{-1} and 0.026 mM^{-1}, respectively. The slope of the calibration curve measured by smartphone spectrometer is ~ 2 times higher than that of plate-reader. In addition, the calibration curves indicate a limit of detection (LOD) of 0.2 mM and 0.47 mM for smartphone and plate-reader, respectively. The LOD is determined as the concentration of analyte at which the signal is 3-fold of standard deviation (3×SD) of blank sample. The limit of quantification (LOQ) was also determined based on 10×SD as 0.8 mM and 1.3 mM for smartphone and plate-reader, respectively. Moreover, the dynamic range for glucose detection is about 0.8-20 mM and 1.3-20 mM for smartphone and plate-reader, respectively. This superior performance might be ascribed to the higher sensitivity of CMOS camera in smartphone as compared to the photodiode detector in the plate-reader. Furthermore, the smartphone spectrometer can monitor the whole spectrum simultaneously in a short time. This is generally not possible with a standard plate-reader, where each spectrum is collected serially by scanning the light across the wavelength range of interest. Thus, the smartphone offers a promising method for rapid monitoring the absorbance changes in real time at potentially higher sensitivity as compared to a commercial bench top plate-reader.

To illustrate the performance of the smartphone spectrometer as LSPR biosensor, an assay for troponin I utilizing AuNPs was designed. LSPR biosensors based on AuNPs and metal nanostructures have been extensively employed for molecular detection.[26] We measured (using this smartphone spectrometer) the absorbance spectra of AuNPs with diameters of 16, 36 and 60 nm that show the LSPR band around 522, 525, 535nm, respectively (see Fig. S4A in Supporting Information). The absorbance spectra are essentially similar to the absorbance spectra measured by UV/Vis spectrometer (see. Fig. S4B), but with a higher noise level.

Peptide-functionalized AuNPs with a diameter of 36 nm were used to detect cardiac human troponin I (cTnI), see Fig.4A. cTnI is present in cardiac muscle tissue as a single isoform with molecular weight 23.8 kDa. For more than 15 years cTnI has been known as a reliable biomarker of cardiac muscle tissue injury and is considered to be more sensitive and specific than the alternative biomarkers used during the last decades – creatin kinase, myoglobin and lactate dehydrogenase isoenzymes.[39]

A specific peptide receptor (CALNN-Peg_4-FYSHSFHENWPS)[1, 40] with high affinity to cTnI was synthesized and immobilized on the surface of 36 nm AuNPs through the cysteine residue (see Supporting Information for the experimental details). In the presence of cTnI, AuNPs aggregate due to bridging of peptides (on separate AuNPs) resulting in a red shift of the LSPR peak. The colour of the AuNPs solution concomitantly changes from red to purple. After extensive aggregation the suspension becomes colourless because of the precipitation of AuNP aggregates to the bottom of the cuvette. The average size of the aggregates formed, as revealed by dynamic light scattering (DLS), also increases with the time of incubation of cTnI (see Fig. S5 in the Supporting Information).

The smartphone spectrometer can be employed for real-time monitoring of the intensity $I_s(\lambda)$ changes at different wavelengths upon the addition of cTnI into the peptide-functionalized AuNP suspension (Fig. S6, Supporting Information). The entire absorbance spectrum $A(\lambda)$ was acquired simultaneously from equation 1. As an example, Fig.4B shows the absorbance spectra $A(\lambda)$ of AuNPs after addition of 2 μg/ml cTnI measured by smartphone spectrometer over time (fitted by Savitzky-Golay method[41]). The overall absorbance of the spectra decreases upon addition of cTnI at a concentration of 2 μg/ml. In addition, after 10-min incubation of cTnI, another peak appears at about 600 nm due to the formation of AuNP aggregates. The average absorbance changes at 540-542 nm (corresponding to location 2 in the colour band, see Fig. S6 in Supporting Information) shows the binding kinetics between the peptide and cTnI (Fig. 4C). The absorbance increase during the first 1-2 min upon the addition of cTnI (at t=~7min) followed by an exponential decrease (Fig. 4C), which is consistent with the spectra changes as indicated in Fig. 4B. From the time-dependent absorbance measurements it is easy to distinguish the response of 500ng/ml and 2μg/ml cTnI. In addition,

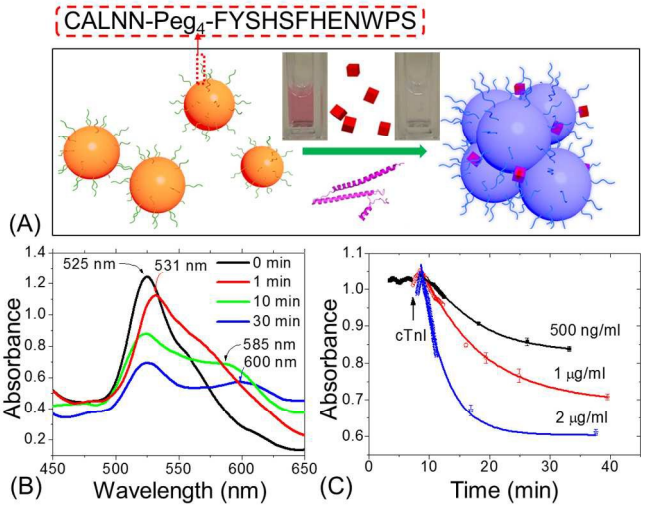

Fig. 4 (A) Schematic illustration of cTnI-induced aggregation of peptide-functionalized AuNPs with the solution changing from red to nearly colourless. (B) LSPR spectra of AuNPs after adding of 2 μg/ml cTnI for 0 to 30 min, recorded by smartphone spectrometer and fitted by Savitzky-Golay method. (C) Time-dependent total intensity changes for three concentrations of cTnI obtained from the smartphone colour band image at 540-542 nm. The data points with error bars were the average absorbance measured in 15 s. The solid lines were fitted with an exponential decay equation, $y=C+Be^{-x/k}$.

the smartphone spectrometer shows the feasibility for real time monitoring of the peak position as well, which is typically not possible with a plate-reader or UV/Vis spectrometer.

The LOD is estimated to be 50 ng/ml (as indicated in Fig. S6D), which is comparable to the one measured on peptide-functionalized planar gold film using a SPR spectrometer (Fig. S7) and a bench top XNano instrument (LOD of 15 ng/ml, see Fig. S8 in Supporting Information). In addition, the noise level of smartphone spectrometer can be further reduced, and the acquisition can also be improved, e.g. through numerical correction of the spectra and better signal evaluation algorithms. [1, 42, 43] Overall, as compared to plate-reader, UV/Vis spectrometer, SPR spectrometer and XNano instrument, our smartphone spectrometer shows comparable and even improved performance. In addition, the smartphone platform is produced from inexpensive components. It is also compact and portable making it suitable for remote biosensing applications and field testing.

Conclusions

We have developed a cheap and portable smartphone spectrometer for monitoring optical changes in real time. The smartphone spectrometer uses the build-in LED as the light source, CMOS camera as detector and a CD grating as the dispersive unit. This standalone phone based spectrometer does not require any external light source, filter, lens and detector. We utilized this smartphone spectrometer to analyse the response from a well-established glucose assay. Interestingly, this smartphone spectrometer shows two-fold higher sensitivity compared to that of commercial plate-reader. Furthermore, we demonstrated the application of this smartphone spectrometer as a LSPR biosensor for the heart disease biomarker, cardiac human troponin I. The smartphone spectrometer enables a fast, sensitive and real-time monitoring of the binding of troponin I. The limit of detection (LOD) for troponin I is comparable to SPR measurement and commercial XNano instrument. The LOD of the smartphone-based sensing system could be further improved by reducing the noise level of this smartphone spectrometer, e.g. by providing advanced data processing algorithms. The smartphone spectrometer shows comparable performance with commercial plate-reader and UV/Vis spectrometer, but it is much cheaper, compact and portable. Additionally, it is capable of monitoring the whole spectrum of sample simultaneously in a short time. We foresee numerous scenarios where the smartphone spectrometer can find applications in, for example, in field testing, lifestyle monitoring and home diagnostics.

Acknowledgements

This work was supported by Science & Engineering Research Council (SERC) of Agency for Science, Technology and Research (A*STAR) under the number of 102 152 0014 and MOE-Tier 1 (2014-T1-001-133-01). We also acknowledge the support from the provost office, and from the ifood and TCT fellowship program of NTU.

Notes and references

[a] *Centre for Biomimetic Sensor Science, School of Materials Science and Engineering, Nanyang Technological University, 50 Nanyang Drive, 637553 Singapore. Tel: 65 6316 2957; E-mail: bliedberg@ntu.edu.sg*
[b] *Wenzhou Institute of Biomedical and Engineering, Wenzhou Medical University, Wenzhou, 325001, PR China*
[c] *Sorbonne Universités, UPMC Univ Paris 6, UMR CNRS 7197, Laboratoire de Réactivité de Surface, F75005 Paris, France*

[‡] Equal Contribution.

† Electronic Supplementary Information (ESI) available: Experimental detail and other results. See DOI: 10.1039/c000000x/

1. R. Halai and M. Cooper, in *Label-Free Biosensor Methods in Drug Discovery*, ed. Y. Fang, Springer New York, 2015, DOI: 10.1007/978-1-4939-2617-6_1, ch. 1, pp. 3-15.
2. D. Mabey, R. W. Peeling, A. Ustianowski and M. D. Perkins, *Nat Rev Micro*, 2004, **2**, 231-240.
3. D. C. Hay Burgess, J. Wasserman and C. A. Dahl, *Nature*, 2006, **444 (S1)**, 1-2.
4. G. M. Whitesides, *Nature*, 2006, **442**, 368-373.
5. C. D. Chin, T. Laksanasopin, Y. K. Cheung, D. Steinmiller, V. Linder, H. Parsa, J. Wang, H. Moore, R. Rouse, G. Umviligihozo, E. Karita, L. Mwambarangwe, S. L. Braunstein, J. van de Wijgert, R. Sahabo, J. E. Justman, W. El-Sadr and S. K. Sia, *Nature Medicine*, 2011, **17**, 1015-U1138.
6. X. D. Zhou, T. I. Wong, H. Y. Song, L. Wu, Y. Wang, P. Bai, D. H. Kim, S. H. Ng, M. S. Tse and W. Knoll, *Plasmonics*, 2014, **9**, 835-844.
7. J. Hu, S. Q. Wang, L. Wang, F. Li, B. Pingguan-Murphy, T. J. Lu and F. Xu, *Biosens. Bioelectron.*, 2014, **54**, 585-597.
8. E. Petryayeva and W. R. Algar, *RSC Advances*, 2015, **5**, 22256-22282.
9. Q. S. Wei, H. F. Qi, W. Luo, D. Tseng, S. J. Ki, Z. Wan, Z. Gorocs, L. A. Bentolila, T. T. Wu, R. Sun and A. Ozcan, *ACS Nano*, 2013, **7**, 9147-9155.
10. Z. J. Smith, K. Q. Chu, A. R. Espenson, M. Rahimzadeh, A. Gryshuk, M. Molinaro, D. M. Dwyre, S. Lane, D. Matthews and S. Wachsmann-Hogiu, *PLoS One*, 2011, **6**.
11. A. Scheeline, *Appl. Spectrosc.*, 2010, **64**, 256A-268A.
12. D. Gallegos, K. D. Long, H. J. Yu, P. P. Clark, Y. X. Lin, S. George, P. Nath and B. T. Cunningham, *Lab Chip*, 2013, **13**, 2124-2132.
13. K. D. Long, H. Yu and B. T. Cunningham, *Biomed Opt Express*, 2014, **5**, 3792-3806.
14. D. Erickson, D. O'Dell, L. Jiang, V. Oncescu, A. Gumus, S. Lee, M. Mancuso and S. Mehta, *Lab Chip*, 2014, **14**, 3159-3164.
15. Q. S. Wei, R. Nagi, K. Sadeghi, S. Feng, E. Yan, S. J. Ki, R. Caire, D. Tseng and A. Ozcan, *ACS Nano*, 2014, **8**, 1121-1129.
16. L. Shen, J. A. Hagen and I. Papautsky, *Lab Chip*, 2012, **12**, 4240-4243.
17. A. Garcia, M. M. Erenas, E. D. Marinetto, C. A. Abad, I. de Orbe-Paya, A. J. Palma and L. F. Capitan-Vallvey, *Sensor. Actuat. B-Chem.*, 2011, **156**, 350-359.
18. P. Preechaburana, M. C. Gonzalez, A. Suska and D. Filippini, *Angew Chem Int Edit*, 2012, **51**, 11585-11588.
19. H. Y. Zhu, O. Yaglidere, T. W. Su, D. Tseng and A. Ozcan, *Lab Chip*, 2011, **11**, 315-322.
20. H. Y. Zhu, I. Sencan, J. Wong, S. Dimitrov, D. Tseng, K. Nagashima and A. Ozcan, *Lab Chip*, 2013, **13**, 1282-1288.
21. I. Navruz, A. F. Coskun, J. Wong, S. Mohammad, D. Tseng, R. Nagi, S. Phillips and A. Ozcan, *Lab Chip*, 2013, **13**, 4015-4023.
22. A. F. Coskun, R. Nagi, K. Sadeghi, S. Phillips and A. Ozcan, *Lab Chip*, 2013, **13**, 4231-4238.
23. H. Y. Zhu, S. Mavandadi, A. F. Coskun, O. Yaglidere and A. Ozcan, *Anal Chem*, 2011, **83**, 6641-6647.
24. H. Yu, Y. Tan and B. T. Cunningham, *Anal Chem*, 2014, **86**, 8805-8813.
25. J. Homola, *Chem.Rev.*, 2008, **108**, 462-493.
26. K. M. Mayer and J. H. Hafner, *Chem. Rev.*, 2011, **111**, 3828-3857.
27. Y. Wang, J. Dostalek and W. Knoll, *Anal Chem*, 2011, **83**, 6202-6207.
28. Y. Wang, W. Knoll and J. Dostalek, *Anal Chem*, 2012, **84**, 8345-8350.
29. A. Patra, T. Ding, G. Engudar, Y. Wang, M. M. Dykas, B. Liedberg, J. C. Y. Kah, T. Venkatesan and C. L. Drum, *Small*, 2015, DOI: 10.1002/smll.201501603, 10.1002/smll.201501603.
30. A. E. Cetin, A. F. Coskun, B. C. Galarreta, M. Huang, D. Herman, A. Ozcan and H. Altug, *Light-Sci Appl*, 2014, **3**.
31. P. Chen, R. Selegard, D. Aili and B. Liedberg, *Nanoscale*, 2013, **5**, 8973-8976.
32. J. Zhang, Y. Wang, T. I. Wong, X. Liu, X. Zhou and B. Liedberg, *Nanoscale*, 2015, DOI: 10.1039/C1035NR03373J.
33. D. Aili, M. Mager, D. Roche and M. M. Stevens, *Nano Lett.*, 2011, **11**, 1401-1405.
34. X. Liu, Y. Wang, P. Chen, Y. Wang, J. Zhang, D. Aili and B. Liedberg, *Anal Chem*, 2014, **86**, 2345-2352.

35. Y. Wang, X. Liu, J. Zhang, D. Aili and B. Liedberg, *Chemical Science*, 2014, **5**, 2651-2656.
36. D. Aili, P. Gryko, B. Sepulveda, J. A. G. Dick, N. Kirby, R. Heenan, L. Baltzer, B. Liedberg, M. P. Ryan and M. M. Stevens, *Nano Lett.*, 2011, **11**, 5564-5573.
37. D. Aili and M. M. Stevens, *Chem. Soc. Rev.*, 2010, **39**, 3358-3370.
38. D. Aili, R. Selegard, L. Baltzer, K. Enander and B. Liedberg, *Small*, 2009, **5**, 2445-2452.
39. A. S. Jaffe, J. Ravkilde, R. Roberts, U. Naslund, F. S. Apple, M. Galvani and H. Katus, *Circulation*, 2000, **102**, 1216-1220.
40. R. Levy, N. T. K. Thanh, R. C. Doty, I. Hussain, R. J. Nichols, D. J. Schiffrin, M. Brust and D. G. Fernig, *J. Am. Chem. Soc.*, 2004, **126**, 10076-10084.
41. P. A. Gorry, *Anal Chem*, 1990, **62**, 570-573.
42. G. J. Nusz, S. M. Marinakos, A. C. Curry, A. Dahlin, F. Hook, A. Wax and A. Chilkoti, *Anal Chem*, 2008, **80**, 984-989.
43. P. Chen and B. Liedberg, *Anal Chem*, 2014, **86**, 7399-7405.